ESY/Merigeologia ja geofysiikka
46/2011
Espoo

Principles of RIM method: EMRE system

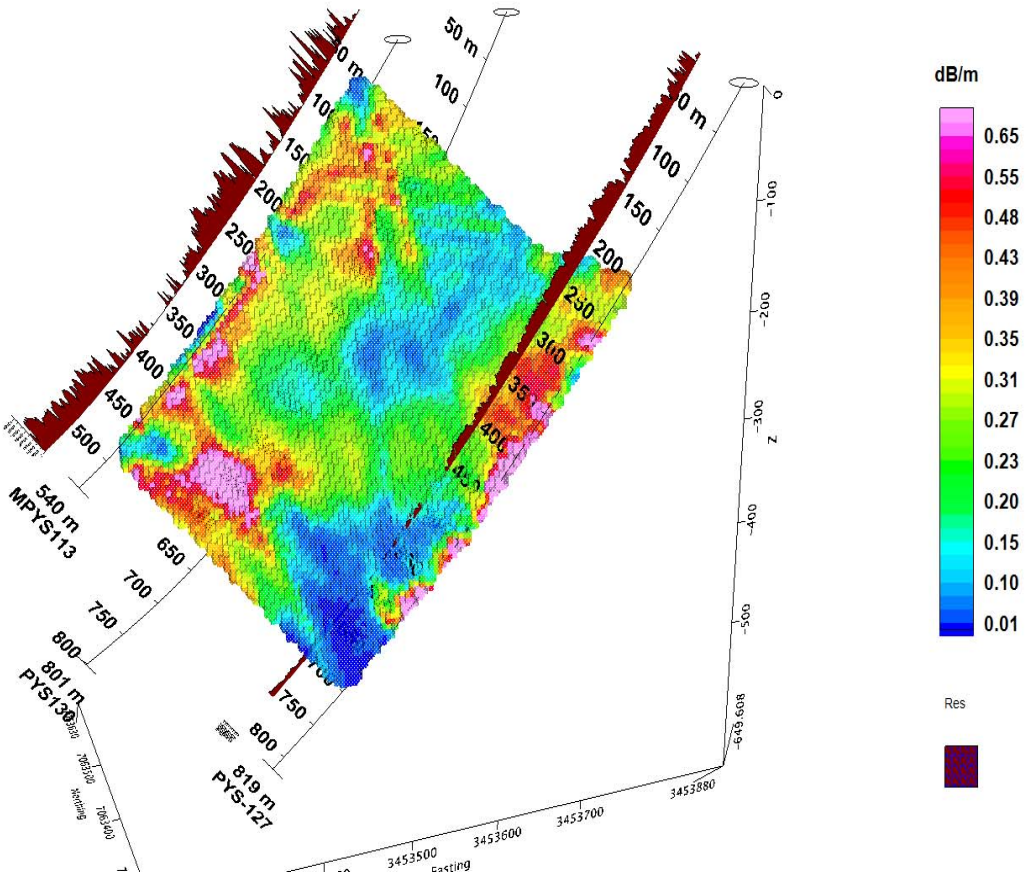

Arto Korpisalo

GEOLOGIAN TUTKIMUSKESKUS • GEOLOGISKA FORSKNINGSCENTRALEN • GEOLOGICAL SURVEY OF FINLAND

PL / PB / P.O. Box 96
FI-02151 Espoo, Finland
Tel. +358 20 550 11
Fax +358 20 550 12

PL / PB / P.O. Box 1237
FI-70211 Kuopio, Finland
Tel. +358 20 550 11
Fax +358 20 550 13

PL / PB / P.O. Box 97
FI-67101 Kokkola, Finland
Tel. +358 20 550 11
Fax +358 20 550 5209

PL / PB / P.O. Box 77
FI-96101 Rovaniemi, Finland
Tel. +358 20 550 11
Fax +358 20 550 14

Y-tunnus / FO-nummer / Business ID: 0244680-7 • www.gtk.fi

GEOLOGIAN TUTKIMUSKESKUS **KUVAILULEHTI**

Päivämäärä / Dnro
07.12.2011

Tekijät	Raportin laji
Arto Korpisalo	Archive report
	Toimeksiantaja

Raportin nimi
Principles of RIM method: EMRE system

Tiivistelmä

A new geophysical borehole prospecting method has been taken into use at the Geological Survey of Finland (GTK), known as the radiofrequency imaging method (RIM). RIM is a high-resolution technique and useful for second-stage explorations and ore body delineations, assisting, e.g. with strategic mine planning and large rock building projects to determine the structural integrity of the rock in the area of interest. It is a computerized tomography method that is based on the radiowave attenuation between the boreholes, making it possible to reconstruct the attenuation distribution of the borehole section (tomogram).

The system consists of a continuous wave (CW) borehole transmitter and borehole receiver. The transmitter and receiver deploy insulated dipole antennas to radiate and receive electromagnetic energy. The borehole transmitter of the system is the hearth where the four measurements frequencies (312.5, 625, 1250 and 2500 kHz) and the vital references frequency (156.25 kHz) are generated. The measurement components are the tangential component of the electric field and the relative phase difference between the measured and reference signal, not being a precise measurement of travel time between the boreholes The reference has its importance in the proper detection of phase difference and amplitude. The measurement or scanning period (movement of the receiver) can be monitored in real time using a portable laptop.

This paper presents the first experiences with the RIM device in Finland, dealing with the technical characteristics of the instrument and comparisons with results measured by other systems (resistivity logging and transient electromagnetic method). Presently, it forms part of the EMRE (ElectroMagnetic Radiofrequency Echoing) system, consisting of the RIM device, an effective graphical interface for data handling, commercial interpretation software and a sophisticated 3D presentation platform for presenting the final results in the borehole environment.

Asiasanat (kohde, menetelmät jne.)
radiofrequency imaging method, RIM, ElectroMagnetic Radiofrequency Echoing, EMRE, cross-borehole geophys-

Maantieteellinen alue (maa, lääni, kunta, kylä, esiintymä)

Karttalehdet

Muut tiedot

Arkistosarjan nimi		Arkistotunnus	
		46/2011	
Kokonaissivumäärä	Kieli	Hinta	Julkisuus
36			julkinen
Yksikkö ja vastuualue		Hanketunnus	
ESY/Merigeologia ja geofysiikka		7780061	
Allekirjoitus/nimen selvennys		Allekirjoitus/nimen selvennys	
Arto Korpisalo			

Sisällysluettelo

1 INTRODUCTION

The radiofrequency imaging method (*RIM*) is a geophysical technique where a bistatic antenna system measures the decayed or attenuated field from a dipole antenna between two deep boreholes at radio frequencies, 100 kHz to 5 MHz. A transmitter is fixed in one borehole while a mobile receiver takes readings in another borehole. The survey is accomplished by transferring the transmitter and receiver in the boreholes. The technique is known as a full tomographic survey (*a two-way measurement*). RIM can be used to scan the subsurface faults, geological contacts and to delineate conductive mineralizations and in mine planning and in determining the structural integrity of the rock.

The first trials to use radio waves to define geological features were taken in the beginning of the 20th century. Stolarczyk (1986) used RIM to detect faults in continuity of seams of coal and this can be kept as a starting point of RIM. The Russian experts made intensive work using RIM with good results during the late 2000's (Buselli, 1980). They measured the decayed or attenuated field and compared it to the theoretically calculated field decay in a homogeneous medium to estimate the conductivity. The Miningtek Pluto-6 system is developed by the Division of Mining Technology of the CSIR (Vogt, 2000). The frequency synthesis ranges from less than 1 Hz up to 30 MHz, and the gain is adjusted effectively to maintain the power at 1 W. The JW-4 system was developed by the Chinese Institute of Geophysical and Geochemical Exploration (*IGGE*). The group used a technique where the cross-sectional image was reconstructed from the ratio of decayed fields at two frequencies (Junxing Cao et al. 2003). In 2010, Geological Survey of Finland (*GTK*) took into a productive use a RIM system, known as the EMRE system.

RIM is based on the attenuation of electromagnetic signals in the region between two boreholes. The summary plot, where the received amplitudes are gathered in the same plot, is an useful and simple way to delineate the possible targets. Using a plane wave assumption (*far-field*),

the measured amplitudes can be converted to the attenuation distribution of the section. Electrical resistivity logging of boreholes is an important exploration technique in identifying mineralised zones in a close proximity to a borehole wall. It is usually the first logging method used on a new borehole. The measurement of resistivity is related to the conductive rock materials near the borehole (Parasnis, 1986). The transient electromagnetic method (*TEM*) is an electromagnetic method (*EM*) functioning in the time domain, in contrast to frequency domain methods (*e.g. RIM/EMRE*). Using TEM, the electrical resistivity of the underground layers can be measured down to a depth of several hundreds of metres. TEM has proved effective for detecting deep anomalies at distances of hundreds of meters from the boreholes (Nabighian & Macnae, 1991).

A comparison of RIM and the resistivity logging method gives the same results under certain circumstances, the conductive zone near the borehole must be conductive enough to be detectable with RIM, but located a little further from the borehole, the logging loses its sensitivity but RIM's ability is even enhanced. When comparing TEM and RIM, the conductive anomaly can be located reliably by the both methods. However, when the distance from the boreholes increases over few hundreds of metres, TEM loses its sensitivity. The depth dimension can also be a restrictive issue with TEM if the loop size cannot be increased. On the contrary, RIM can be used all along the borehole and at the distances where the boreholes are separated by even one thousand metres. The results of the logging method and TEM are usually presented as curves but in RIM, the reconstructed attenuation distribution of a section can be presented as a visual and informative image of frequency dependent response of the subsurface materials to the propagating of electromagnetic energy at a used radio wave frequency band.

2 CONTINUOUS WAVE AND SUPERHETERODYNE TECHNIQUE

Electrical radio communication can be accomplished by two principal means, *radio and wire*. Electromagnetic waves are used in radio communication without any physical guiding path, but communication by wire requires conductors to carry the waves. Modern radio transmitters include continuous wave (*CW*), amplitude-modulated (*AM*), frequency-modulated (*FM*) types. The CW-type was the first to be developed, and is still used in long-range communication. The narrow bandwidth, making it possible to use minor power supplies, is also one of its advantages (Holloway, 1998). The EMRE system consists of borehole devices that are based on the Russian inventions (Redko et al. 2000a) (Fig 1).

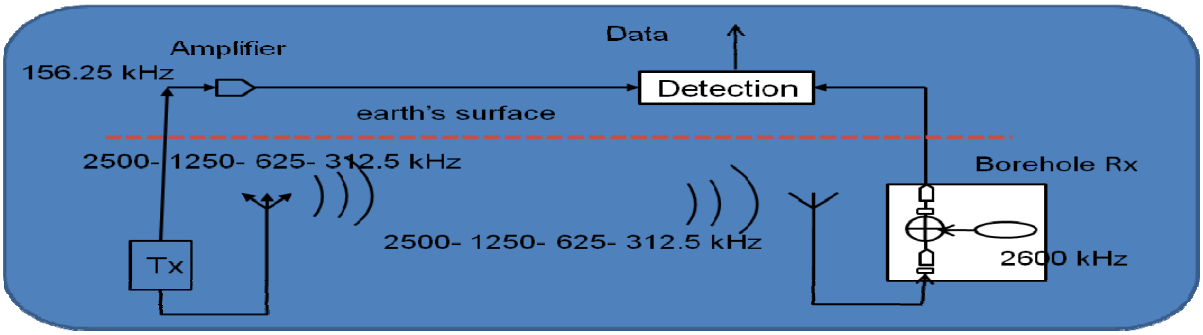

Figure 1. *The diagram of the EMRE system.*

The main components of the transmitter (*CW-device*) are a generator (*oscillator*), a division circuit (*F/1-2-4-8*), amplifiers and an antenna (Fig. 2). The generator is the heart, generating the required base frequency. The voltage and power amplifiers are the means to amplify the oscillations and the antenna is used to radiate electromagnetic waves.

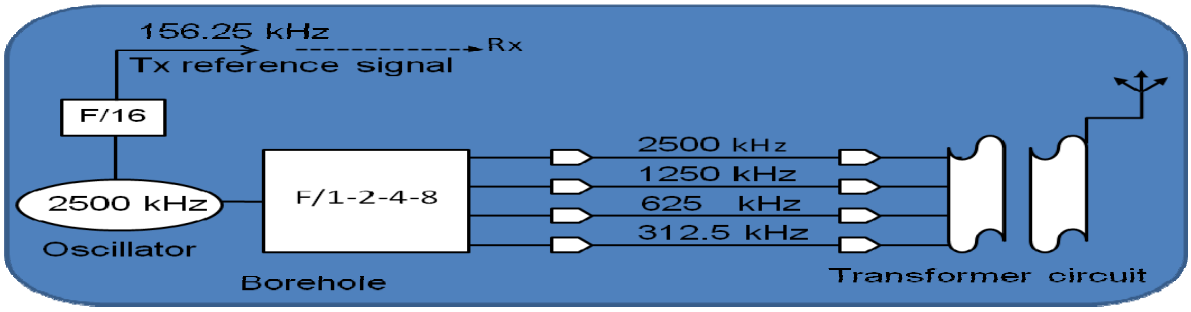

Figure 2. *The diagram of transmitter.*

Figure 2 presents a block diagram of a CW device. The oscillator (*e.g. quartz crystal*) generates the radiofrequency (*RF*) carrier at the basic frequency of 2500 kHz, maintaining it accurately. The other frequencies are generated from a basic frequency in a frequency divider circuits (*F/1-2-4-8/ and F/16*). Before the transmission the voltage and power must be amplified. Applying a transformer circuit, the RF signals are sent to the antenna. Thus, the antenna's function is to serve as an interface between the generator and the surrounding environment.

The first receiver techniques generated problems, but after the development of superheterodyne receivers, most of the problems were overcome. In the superheterodyne receiver, the incoming signal frequency is changed to a lower frequency, known as the intermediate frequency (*IF*) and the major part of the amplification takes place at IF frequency before detection. The receiver processes signals by performing certain basic functions such as *reception, selection and detection.* It has some general and important characteristics, namely *sensitivity, low noise level, selectivity and fidelity*. The sensitivity of a receiver is the minimum RF signal level that can be detected. The best way to improve the sensitivity of a receiver is to reduce the noise level (*e.g. reducing temperature, bandwidth*). Selectivity, receiver's ability to discriminate the wanted signals, is the most important feature for sensing small signals in the presence of strong interferences. Fidelity is a measure of the ability of a receiver to reproduce the original source information. The dynamic range of a receiver is the input power range over which the receiver is useful. In principle, the EMRE receiver consists of two receivers: one is in the borehole and the other at the surface.

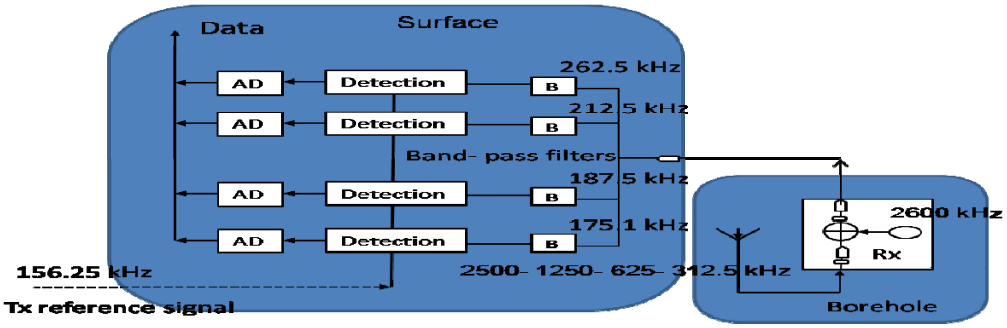

Figure 3. *The diagram of receiver.*

Figure 3 presents the diagram of the receiver. The incoming radiofrequency (*RF*) signals are applied to the band-pass filter and RF amplifier. The RF amplifier improves the signal-to-noise ratio and provide a sufficient selectivity, and it determines the sensitivity of the receiver. This stage is also known as a preselector stage (*the front end of the receiver*). The RF amplifier and a local oscillator are connected in a circuit called a mixer. The signals from the preselector and the unmodulated signal from a local oscillator are heterodyned, producing, e.g. the four constant difference frequencies (*100- 50- 25- 12.5 kHz)* and their harmonics. The constant frequencies of the converted signal are known as the IF frequencies. The mixer stage is also known as a first detector stage. The band (*100- 12.5 kHz*) is several octaves. In the EMRE system, data is transferred from the borehole to the surface using a pair cable where the two filters (*transformers*) are connected. Because it is challenging to transfer effectively the broad first intermediate band through the filters (*inductance*), another mixing stage is performed, using 162.5 kHz (*2.6 MHz/16*) to produce the second intermediate frequencies of 262.5,- 212.5, 187.5 and 175.1 kHz. This band is not even one octave, and the data transfer is not so challenging. The IF signals are applied to the band-pass filter and IF amplifier where the amplified IF signals are passed to the detection stages, one for each frequency. The receiver is tuned or locked to the reference signal (*156.25 kHz*), providing the production of the relative phases and amplitudes. Thus, in the EMRE system, the first detection stage is carried out in the borehole unit, the winch cable is used as a guiding path for the IF signals to the surface where the final detection is performed.

3 THEORY

Computerized axial tomography (*CT*) is a widely used imaging technique and has a very important role in modern medicine and geophysics (*e.g. seismic tomography*). Simple and fast image reconstruction methods are applicable to imaging situations where the line integrals of a parameter are available or the total attenuation along a raypath can be defined as $\alpha_{tot}=\int\alpha dl\approx\sum\alpha_i\cdot l_i$. Geophysical tomography differs from CT in both physical scale and scanning geometry. In geophysics, a larger physical scale is required. In addition, to achieve sufficient signal levels over working distances, much lower frequencies must be used. The spatial resolution in images from geophysical signals may be in the order of tens of metres, while medical images are on millimetre scale. Medical scanning takes place within a fixed data collection geometry. Conversely, in borehole geometry, a new scanning capability is required for each separate measurement (Dines, 1979).

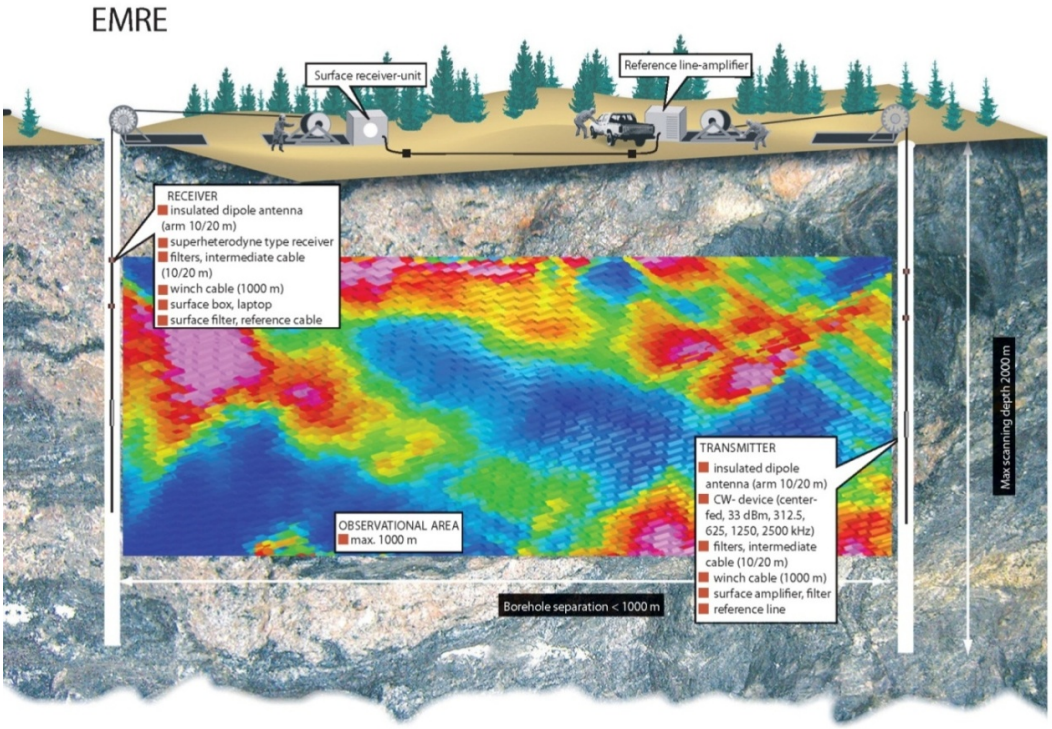

Figure 4. *The radiofrequency imaging method (RIM/EMRE) between two boreholes (not to scale).*

Electromagnetic tomography delineates the geological structures of a cross-borehole section with electromagnetic waves that are transmitted between probes moving up and down the boreholes (Fig. 4). The radiofrequency imaging method (*RIM*) was developed in the early 1980's to detect hazards or obstructions in coal panels prior to long-wall mining (Stolarczyk & Fry, 1986). The method was successful because the coal seam, having electrical resistivity substantially greater than in the surrounding geology, acted as an EM wave-guide. Recently, the technique has been applied in cross-borehole imaging mode, and also successfully operated in a crystalline bedrock environment in exploration (Korpisalo, 2010d; Korpisalo & Niemelä, 2010e; Korpisalo, 2008; Redko et al., 2000b; Stevens et al., 1998).

A cross-borehole EM survey has several clear benefits over the ground-level electromagnetic sounding methods. Applying a borehole source brings the survey closer to the target, and allows the usage of higher frequencies, thus enabling a higher resolution. Another benefit is the possibility to view the target from different angles and directions, not only in a vertical direction and from above. Moreover, the presence of the transmitter in the borehole eliminates boundary effects due to the ground surface and the strong attenuation of EM signal emerging from soil deposits. A drawback is the suboptimal availability and location of boreholes and limited transmission power of the borehole probe. Thus, the relatively complex behaviour of the 3D source field within the subsurface target is difficult to resolve numerically without significant approximations.

The physical behaviour of an electromagnetic field (*EM*) is governed mathematically by Maxwell equations, which describe the relationship between electric (*E*) and magnetic fields (*B*) in a medium and quantify the material's physical properties. This article considers these basic characteristics of the equations using a plane wave assumption which is justified when the point of consider is in far-field domain (Korpisalo, 2010b).

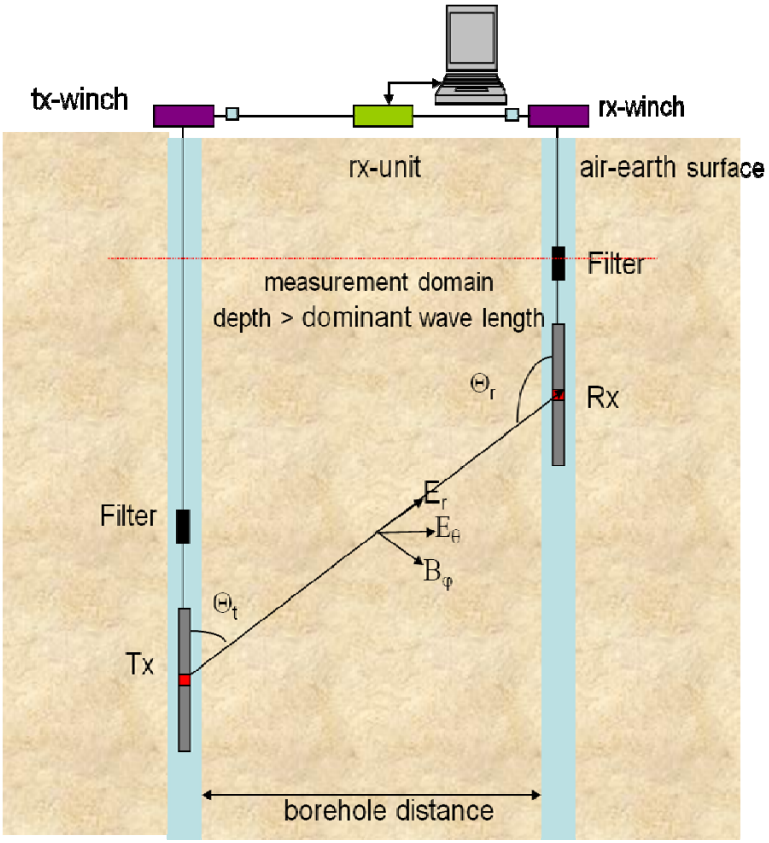

Figure 5. *Schematic drawing of the transmitter and receiver dipoles and the dominant components of electric field E and magnetic field B of the electric dipole. The tangential component* E_Θ *is the dominant component in the far-field domain, where the radial component* E_r *is diminishing.*

The form of an electromagnetic wave is dependent on the nature of the material in which the wave is propagating. The simplest waves in a homogeneous medium are uniform plane waves that are at a large distance from the source, having negligible curvature over a limited area, and are called transverse electromagnetic waves (*TEM-waves*). TEM-waves have only transverse electric and magnetic field components and no longitudinal component in the direction of propagation or in the direction of power flow (*Poynting vector* $\hat{S}$) or $\hat{S} = \frac{1}{2}\overline{E} \times \overline{H}'$ where $\overline{H}'$ is the complex conjugate of the magnetic field. Plane waves are the simplest way to apply the neces-

sary equations and indeed, at large distances from the source, the waves have negligible curvature and can be represented by plane waves over a limited area.

The four electromagnetic equations that explain the field characteristics are:

$$\nabla \cdot \overline{D} = \rho \qquad (\textit{Gauss', electricity}) \qquad (1)$$

$$\nabla \cdot \overline{B} = 0 \qquad (\textit{Gauss' law, magnetism}) \qquad (2)$$

$$\nabla \times \overline{E} = -\frac{\partial \overline{B}}{\partial t} \qquad (\textit{Faraday's law}) \qquad (3)$$

$$\nabla \times \overline{H} = \overline{J} + \frac{\partial \overline{D}}{dt} \qquad (\textit{Ampere's law}) \qquad (4)$$

The expressions for an electromagnetic wave propagating in a linear, isotropic, homogeneous and stationary medium can be derived from these four equations. The notation used in the above equations is: D=electric displacement [C/m^2], E= electric field intensity [V/m], B=magnetic induction [T], H=magnetic field intensity [A/m], J=electric current density [A/m^2], ρ=free charge density [C/m^3].

The material properties determine the relationships between vector fields in Maxwell's equations, and the constitutive equations can be written in a linear, homogeneous and isotropic medium as

$$\overline{D} = \varepsilon \cdot \overline{E}$$

$$\overline{H} = \overline{B} / \mu \qquad (5)$$

$$\overline{J} = \sigma \cdot \overline{E}$$

where ε is electrical permittivity, determining the ability of the medium to store and release electromagnetic energy (*like the storage ability of a capacitor*), or it can be described as the degree of polarization in the medium; μ is magnetic permeability and describes how atomic and molecular magnetic moments respond to the magnetic field; and σ is electrical conductivity, which describes the medium's ability to transmit free electric charges (*electrons or ions*). All these parameters are scalar constants under the conditions stated above. Using Eq. 5, Faraday's and Ampere's law can be written as

$$\nabla \times \overline{E} = -\mu \frac{\partial \overline{H}}{\partial t} \tag{6}$$

$$\nabla \times \overline{H} = \sigma \overline{E} + \varepsilon \frac{\partial \overline{E}}{dt} \tag{7}$$

Taking the curl of Eq. 7 and substituting the result in Eq. 6, the inhomogeneous generalized time-domain wave equations for E and H are derived:

$$\nabla^2 \overline{E} - \mu\sigma \frac{\partial \overline{E}}{dt} - \mu\varepsilon \frac{\partial^2 \overline{E}}{\partial t^2} = \frac{1}{\varepsilon} \nabla \rho + \mu \frac{\partial \overline{J}}{\partial t} \tag{8}$$

$$\nabla^2 \overline{H} - \mu\sigma \frac{\partial \overline{H}}{dt} - \mu\varepsilon \frac{\partial^2 \overline{H}}{\partial t^2} = -\nabla \times \overline{J} \tag{9}$$

On the right hand-side are the sources of the fields. On the left-hand side, the second-order time-derivative term is the wave term (*oscillating term*) with an energy storage factor ($\mu\varepsilon$) and the first-order time-derivative term is the damping term with an energy dissipation factor ($\mu\sigma$). For sinusoidal time-harmonic fields ($e^{i\omega t}$), these equations (*in a source-free region, ρ=0 and J=0*) become frequency-domain *Helmholtz's equations.* Using the following substitutions; $\frac{\partial}{\partial t} \to i\omega, \frac{\partial^2}{\partial t^2} \to -\omega^2$, Eq. 8 and Eq. 9 can be written as

$$\nabla^2 \overline{E} - i\omega\mu\sigma \overline{E} + \omega^2 \mu\varepsilon \overline{E} = 0 \to \nabla^2 \overline{E} + k^2 \overline{E} = 0 \tag{10}$$

$$\nabla^2 \overline{H} - i\omega\mu\sigma \overline{H} + \omega^2 \mu\varepsilon \overline{H} = 0 \to \nabla^2 \overline{E} + k^2 \overline{E} = 0 \tag{11}$$

where $k^2 = \omega^2 \mu\varepsilon - i\omega\mu\sigma$ is the complex wave number and $i = \sqrt{-1}$ an imaginary unit. With an assumption of low conductivity and high frequencies we obtain the homogeneous wave equations

$$\nabla^2 \overline{E} - \omega^2 \mu\varepsilon \overline{E} = 0 \to \nabla^2 \overline{E} - k^2 \overline{E} = 0 \tag{12}$$

$$\nabla^2 \overline{H} - \omega^2 \mu\varepsilon \overline{H} = 0 \to \nabla^2 \overline{H} - k^2 \overline{H} = 0 \tag{13}$$

where $k^2 \approx \omega^2 \mu\varepsilon$. With a high conductivity and low frequencies, Eq. 10 and Eq. 11 become diffusion equations

$$\nabla^2 \overline{E} - i\omega\mu\sigma\ \overline{E} = 0 \rightarrow \nabla^2 \overline{E} - k^2 \overline{E} = 0 \tag{14}$$

$$\nabla^2 \overline{H} - i\omega\mu\sigma\ \overline{H} = 0 \rightarrow \nabla^2 \overline{H} - k^2 \overline{H} = 0 \tag{15}$$

where $k^2 \approx -i\omega\mu\sigma$ or $k = (1-i)\sqrt{\omega\mu\sigma/2}$. Now $\overline{E}$ and $\overline{H}$ are damping or decaying fields rather than waves (*quasi-static fields*). The Q-factor defined by $Q = \frac{\omega\varepsilon}{\sigma}$ (*inverse loss tangent*) is an important constant that describes the characteristic of field behaviour. When Q>>1, energy storage effects associated with permittivity (ε) and permeability (μ) are dominant (*fields are propagating*). When Q<<1, energy loss effects associated with conductivity (σ) are dominant (*fields are diffusing*). The second and third terms in Eqs. 10- 11 represent the electrical conduction and displacement. In a plane wave the fields propagate in a direction that is perpendicular to the plane of the wave. This is also known as the wave front, in which the front is an equi-amplitude plane, meaning that the field strength is constant on the plane. In the case of a linearly x-polarized wave propagating in the positive z-direction (*E directed along the x-axis*), the solutions to Eq. 10 and Eq. 11 are

$$\overline{E} = E_o \exp(\ i\omega t - \gamma z\ )\hat{x} \tag{16}$$

$$\overline{H} = H_o \exp(\ i\omega t - \gamma z\ )\hat{y} \tag{17}$$

where γ is the constant of propagation

$$\gamma^2 = i\omega\sigma\mu + i^2\omega^2\mu\varepsilon \ \ or\ \ \gamma = i\omega\sqrt{\mu\left(\varepsilon - i\frac{\sigma}{\omega}\right)} = i \cdot k \tag{18}$$

Normally, γ is a complex function of the electromagnetic material parameters ε, σ, μ and ω (*angular frequency*). Eq. 18 is in the form of

$$\gamma = \alpha + i\beta \tag{19}$$

Thus, Eq. 16 and 17 can then be written as

$$\overline{E} = E_o \exp(\, i(\omega t - \beta z) - \alpha z)\hat{x} = E_o \exp(\, i(\omega t - \beta z)) \exp(\, -\alpha z)\hat{x} \quad (20)$$

$$\overline{H} = H_o \exp(\, i(\omega t - \beta z) - \alpha z)\hat{y} = H_o \exp(\, -i(\omega t - \beta z)) \exp(\, -\alpha z)\hat{y} \quad (21)$$

$$\overline{H} = \frac{E_o}{\eta} \exp(\, i(\omega t - \beta z) - \alpha z)\hat{y} \quad (22)$$

where η is the wave impedance or $\eta = \sqrt{\frac{\mu}{\varepsilon}}$. In free space, $\eta \approx 377\Omega$ and the electric and magnetic fields are in phase. In a dissipative medium, the wave impedance is a complex quantity and the electric and magnetic fields are no longer in phase, thus a complex power flow density is established or the Poynting vector can be written as $\hat{S} = 1/2 \cdot \left(\overline{E} \times \overline{H}'\right) = \overline{S} + i\overline{q}$, where $\overline{S}$ is the active component (a*verage power component in flow*) and the imaginary component $\overline{q}$ is the reactive component of complex power density. Thus, a Poynting vector having only a reactive component does not transfer power at all, but electric and magnetic energy is stored in the near field of the antenna and it is the active component that contributes to the power transfer. As can be seen from Eqs. 20- 21, the amplitudes and phases of the fields are controlled by the terms αz and βz. The first exponential function is the propagation term and the second is the attenuation (*damping*) term, where α is the attenuation constant and β is the phase constant. The general expressions for β and α can be written as (Korpisalo, 2010b)

$$\beta = \omega\sqrt{\frac{\mu\varepsilon}{2}}\left(\sqrt{1+\left(\frac{\sigma}{\omega\varepsilon}\right)^2}+1\right)^{1/2} = \omega\sqrt{\frac{\mu\varepsilon}{2}}\left(\sqrt{1+\tan^2\Phi}+1\right)^{1/2}(rad/m) \quad (23)$$

$$\alpha = 8.686 * \omega\sqrt{\frac{\mu\varepsilon}{2}}\left(\sqrt{1+\left(\frac{\sigma}{\omega\varepsilon}\right)^2}-1\right)^{1/2} = 8.686 * \omega\sqrt{\frac{\mu\varepsilon}{2}}\left(\sqrt{1+\tan^2\Phi}-1\right)^{1/2}(dB/m) \quad (24)$$

where $\tan\Phi$ is referred as loss tangent. In weakly lossy dielectric (*high frequencies, tanΦ<<1*), Eqs. 23- 24 can be simplified as $\beta \approx \omega\sqrt{\mu\varepsilon}$, $\alpha \approx 8.686 \cdot \frac{\sigma}{2}\sqrt{\mu/\varepsilon}$. In good conductors (*low frequencies, tanΦ>>1*), the attenuation constant is equal to the phase constant or $\alpha = \beta = \sqrt{\omega\mu\sigma/2}$. Now, $\beta = \sqrt{\pi f\mu\sigma}$, $\alpha = 8.686\sqrt{\pi f\mu\sigma}$. At distance $\delta = 1/\alpha$, the field has attenuated to a fraction e^{-1} of the initial field strength. The distance is known as the skindepth (Korpisalo, 2010b). Table 1 presents the skindepths (*D*) and attenuation constants (*dB/m*) with different material properties.

Table 1. *The skindepths (D) and attenuations (dB/m) with different material properties*.

Resistivity	2500 Ωm				7500 Ωm				15000 Ωm			
kHz	312.5	625	1250	2500	312.5	625	2500	2500	312.5	625	1250	2500
D (m)												
ε_r= 10	55	44	42	42	133	126	126	126	256	252	252	252
ε_r= 40	87	84	84	84	252	252	252	252	504	504	504	504
dB/m												
ε_r= 10	0.16	0.20	0.20	0.20	0.065	0.068	0.068	0.068	0.034	0.034	0.034	0.034
ε_r= 40	0.10	0.10	0.10	0.10	0.034	0.034	0.034	0.034	0.017	0.017	0.017	0.017

4 EMRE INSTRUMENT

In Finland, the RIM method has been used since 2005 (Korpisalo, 2005; Korpisalo, 2008). The heart of the system is a CW transmitter (*a continuous wave device*), which simultaneously operates at a maximum of four frequencies; 312.5, 625, 1250 and 2500 kHz (Fig. 5). The survey time is reduced by measuring all frequencies simultaneously. The transmitter power (*2 W/33 dBm*) is divided between the frequencies; thus, the highest power is obtained using a single frequency. The borehole cables (*electric dipole antenna + intermediate cable*) are 40/50 m long. The transmitter antennas consist of a 36 mm tube for the corresponding electronics and a voltage source 1.5 m in length (*receiver probe 2.5 m in length*). The antennas are slim 6 mm dipole antennas (*insulated antennas aligned with the borehole axis, arm lengths being 10 or 20 m*) to radiate electromagnetic waves into the bedrock. The same types of antennas are used in receiving the electromagnetic energy.

The measurements can be done using MOM *(Multi Offset Measurement*) or ZOM (*Zero Offset Measurement*) technique. The MOM is the traditional way where a stable transmitter is fixed in one borehole and a mobile receiver is moving in the other borehole (*fan-beam geometry*). The main idea is to measure a large number of angles passing through the space between the boreholes. In the ZOM measurement both the transmitter and receiver are moving synchronously in the boreholes (*parallel-beam geometry*). This is a quick and simple technique to locate and define anomalous attenuation zones. In a homogeneous environment signal levels should be same at each location. Normally, the measurement is performed as a two-way measurement where the transmitter and receiver are interchanged in the boreholes. Thus, a full tomographic survey can be accomplished.

The amplitudes of the electric field (*~tangential component of electric field in the far-field domain*) along the receiver borehole axis and the relative phase difference (*between the reference signal and received signals*) and are measured (Fig. 5). A reference signal is generated in the

transmitter borehole unit and fed through cables to the receiver unit at the earth's surface. This is an essential signal when tuning the receiver, but even if tuning is not functioning properly, the equipment can be used to register the amplitudes strongly enough, because the signals maintain the basic trend lines, although the amplitude levels are wrong, also meaning misleading attenuation levels. In addition, the reference signal considerably improves the sensitivity and noise immunity of the tool. Special filters are used to isolate antennas galvanically from winch cables. Measurements are controlled and information is recorded with a portable computer. Scanning speeds (*receiver movement*) can be as high as 30 m/min without any disturbance. The automated measurement process requires minimal intervention by the operator. The operator can monitor the data quality at all the frequencies in real time or view previous results. This allows adjustments to the survey depth range and sampling density, and will enable decisions on re-measurement (Figs. 4- 5). Both winch cables are 1000 m in length. The technical specifications of the RIM system are presented in Table 2. Figure 6 presents the main parts of the measurement system.

Table 2. *Technical specifications of the system. (MOM-Multi-Offset Measurement, ZOM -Zero Offset Measurement*).

Operating frequencies	312.5, 625, 1250, 2500 kHz
Measument range of voltage	0.5-1000 μV
Measument range of phase	0-360°
Maximal transmitter power	2W(33dBm)
Diameter of downhole probe	36 mm
Measurement modes	ZOM and MOM
Winch capacity	1000 m
Pressure tolerance	<2000 m

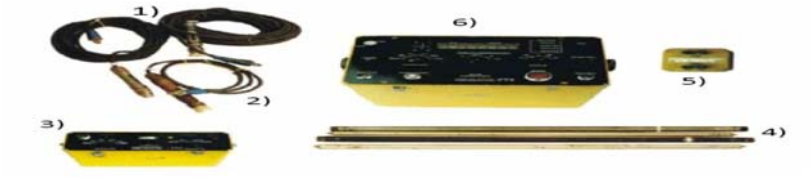

Figure 6*. EMRE instrumentation; antennas (1); intermediate cables (2); transmitter unit (3) serving as an amplifier for the reference signal; transmitter and receiver casings (4); surface filter (5); receiver surface control unit (6).*

5 PRELIMINARY TESTS

Despite the equipment being designed to operate in far-field conditions in deep boreholes, some tests can be performed in order to check the proper functioning of the transmitter and receiver. It is also good to occasionally test the calibration system. Because the EMRE system works also in the near-field domain (*mutual coupling between units is strong and unavoidable*) within laboratory environments, the changes in amplitudes and phase may be significant. A detailed description of items that can be checked before the fieldworks is provided by Korpisalo (2007).

The calibration unit is internal and signals (*1μV, 10μV, 100μV*) can be fed directly to the receiver antenna input using the four measurement frequencies. Assuming that the induced voltage is proportional to the component of the electric field parallel to the axis of the antenna, knowledge of material parameters is not necessary at every location where the antenna is situated, but a single calibration in one material is sufficient. This is also a simple way to check the system and ensure that the receiver is functioning correctly. The user should see the responses of the receiver to the transmitted signal strengths as a step function (Figs. 7- 8).

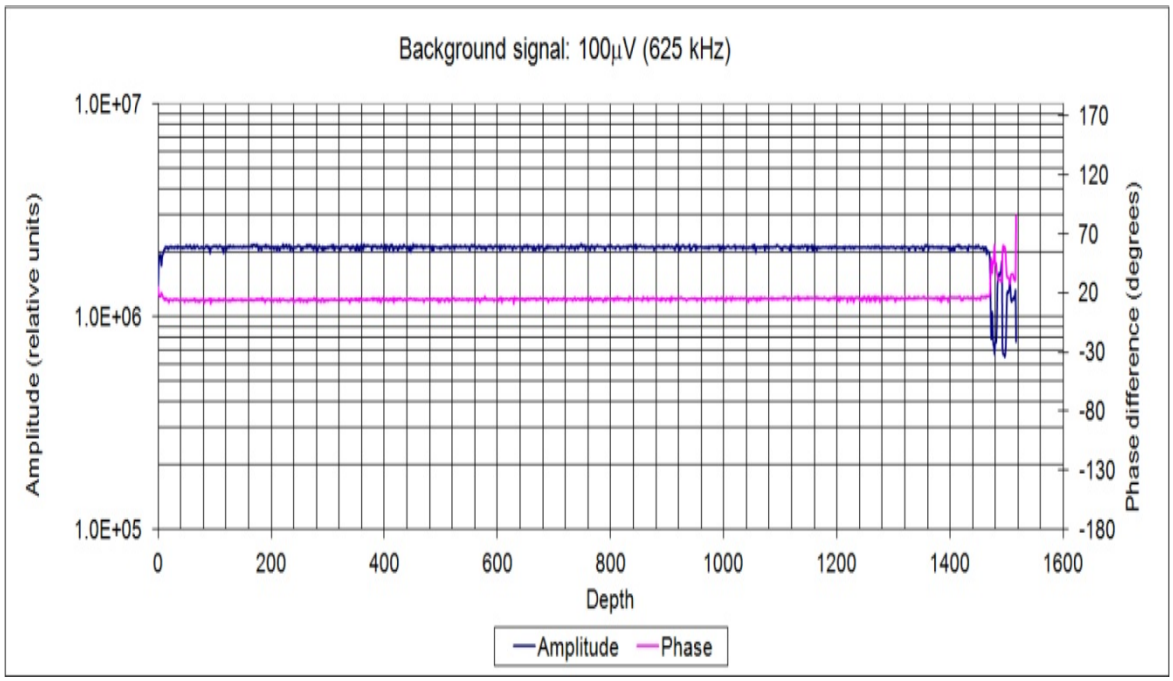

Figure 7. *The responses of the calibration signal of 100 μV (amplitude and phase difference).*

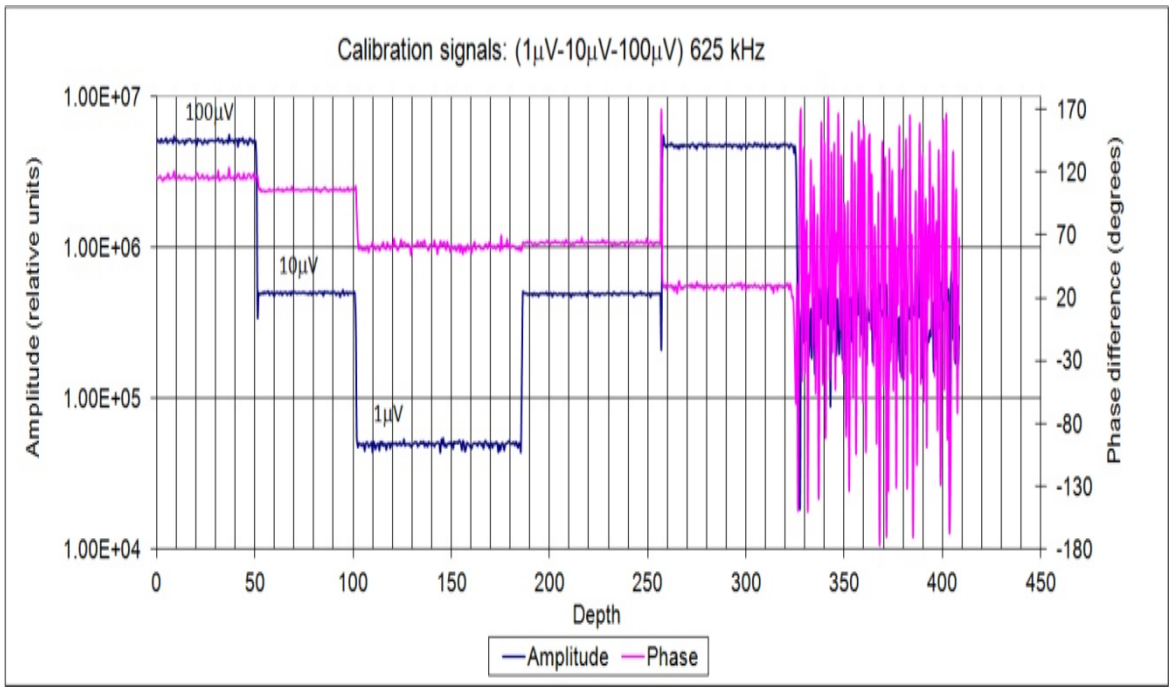

Figure 8. *Responses of three constant calibration signals (1μV-10μV-100μV) at 625 kHz. Tuning is disturbed after the 325 m level or the receiver is not locked to the reference signal.*

6 FIELD MEASUREMENTS AND COMPARISONS

Working in a cross-borehole mode (*transmission*), the transmitter (*tx*) and receiver (*rx*) probes are situated in different boreholes and the system is referred to as bistatic. To avoid earth-surface reflections, the starting depth must be greater than one dominant wavelength (λ) in rock (Table 3) where ρ is the resistivity and ε_r the relative permittivity.

Table 3. Typical wavelengths with different material properties.

Frequency (kHz)	Wavelength (λ) ρ= 10000 Ω ε_r= 10	Wavelength (λ) ρ= 1000 Ω ε_r= 10	Wavelength (λ) ρ= 100 Ω ε_r= 10
312.5	~300 m	~180 m	~70 m
625	~110 m	~100 m	~40 m
1250	~80 m	~70 m	~30 m
2500	~40 m	~40 m	~20 m

However, according to our first experiments, it is possible in some situations to start even closer to the earth's surface without disturbing the receiver (Fig. 5). In particular, when the transmitter is below the recommended starting depth, the receiver may also be used at shallower depths. Naturally, amplitudes diminish due to the distance between Tx and Rx (*geometric scattering*), but strong changes due to internal attenuation of the surrounding materials are also evident. Higher frequencies mean higher attenuation. Other issues may also have a strong effect on the transmitter efficiency, reducing the radiation power from the antenna. The scattering parameter s_{11} in the transmitter (Fig. 9) is an important factor that defines the relationship between the reflected and input power of the transmitter generator, and it can make the functioning of the

transmitter almost impossible with a fixed frequency (Korpisalo, 2010a). The dipole locations are presented in Figure 10.

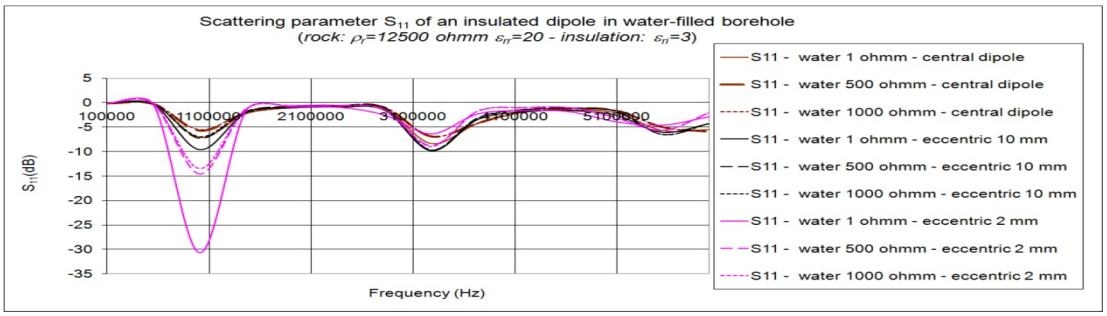

Figure 9. *The behaviour of scattering parameter s_{11} in the transmitter. The highest system frequency (2500 kHz) suffers most in this situation, causing the transmitter antenna to function ineffectively. Rock's resistivity is 12500 Ωm and permittivity ε_{rr}=20. The permittivity of insulation is ε_{rr}=3.*

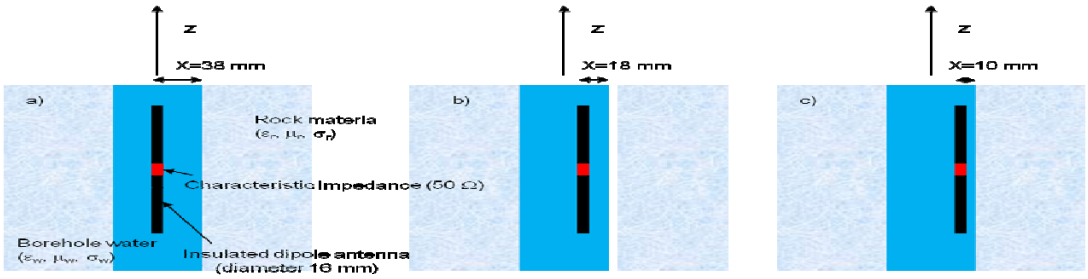

Figure 10. *The dipole locations in the borehole. a) In a central position and the outer surface of the antenna is 30 mm from the borehole wall (insulation Ø16 mm, borehole Ø76 mm). b) In eccentric 10 mm model, the outer surface is 10 mm from the borehole wall. c) In eccentric 2 model, the outer surface is 2 mm from the borehole wall.*

A typical registration of amplitude (*not normalized*) and phase difference at *625 kHz* are displayed in Figures 11-12. The stationary transmitter was in borehole PYS127 (*410 m*) and the mobile receiver in borehole MPYS113 at the Pyhäsalmi volcanic complex (*PVC*) (*Ruotanen formation/Kettuperä member*). Ruotanen formation is bimodal (Mäki, 1986) with felsic rocks and mafic rocks (Kousa et al., 1994). The Massive Sulphide deposits (VMS) are often associated to these bimodal volcanic environments. VMS deposits are an important source of Zn, Cu, Pb,

Ag and Au. Pyrite is generally the most abundant subordinated amounts of chalcopyrite, sphalerite and galena. Magnetite can be present in minor amounts. The base metals zinc and copper are the two most important commodities produced from most VMS deposits. The Kettuperä member has been defined on the basis of drill hole data (there are no outcrops). Large changes in amplitude occur at the level of 350 m (Fig. 11), which are continued by the total disappearance of the signal to noise level after 400 m, where phase detection hardly functions (Fig. 8). The receiver was shadowed by a strong attenuator in MPYS113 (Fig. 15). Possible multipath reflections (*Rayleigh scattering*) can be seen starting from the level of 442 m (Fig. 12), where the device has sensed stronger signals through longer paths (*~130^o phase change*). In both figure, the amplitudes may also have local increasing trends, this means that signals have penetrated to the receiver through more resistive channel.

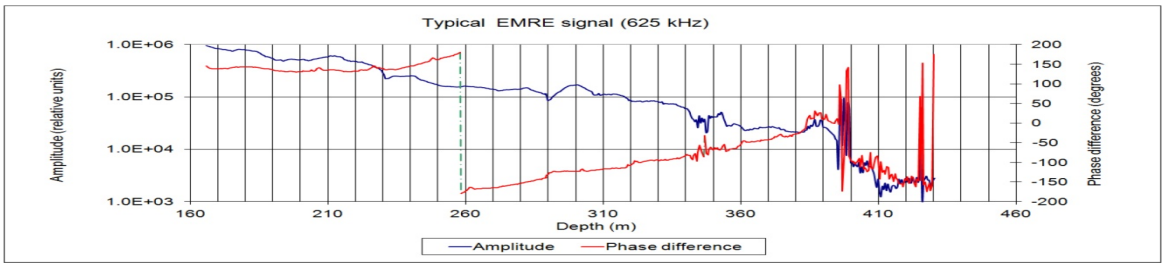

Figure 11. *Typical measurement registration at a frequency of 625 kHz. Depth readings are cable lengths in the boreholes. Due to the presentation mode, the phase is plotted between -180^o and +180^o.*

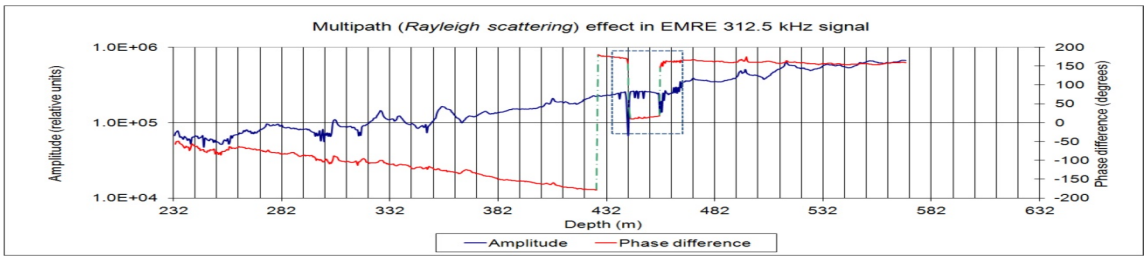

Figure 12. *Possible multipath wave (Rayleigh scattering) effect at 442-455 m. The phase has suddenly changed ~130 degrees, meaning a path ~2/5 of a wavelength longer than a direct wave (one wavelength (λ) means a phase shift of 2π radians . Due to the presentation mode, the phase is plotted between -180^o and +180^o.*

In Figures 13-14, normalized amplitudes (*Tx-Rx distance*) are plotted. The transmitter depth ranges from 160 m to 210 m in PYS127 and correspondingly from 150 m to 180 m in MPSY113. Bold signals are received in borehole PYS127, and dashed signals respectively are received in MPYS113. The measurement frequencies are 312.5, 625, 250, 2500 kHz.

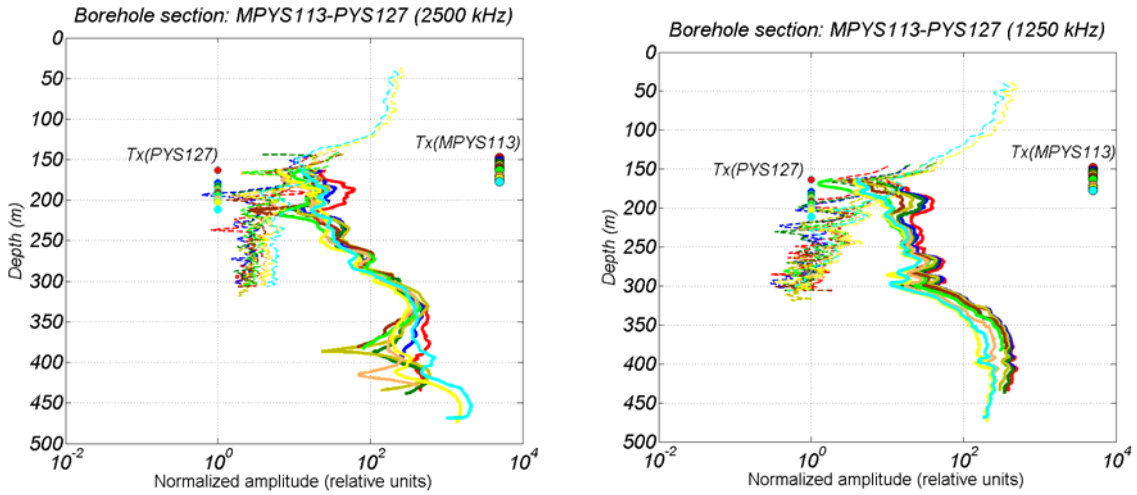

Figure 13. *The normalized amplitudes measured in boreholes PYS127 (bold lines) and MPYS113 (dashed lines). Corresponding transmitter positions are marked with coloured circles. Depths are real vertical depths.*

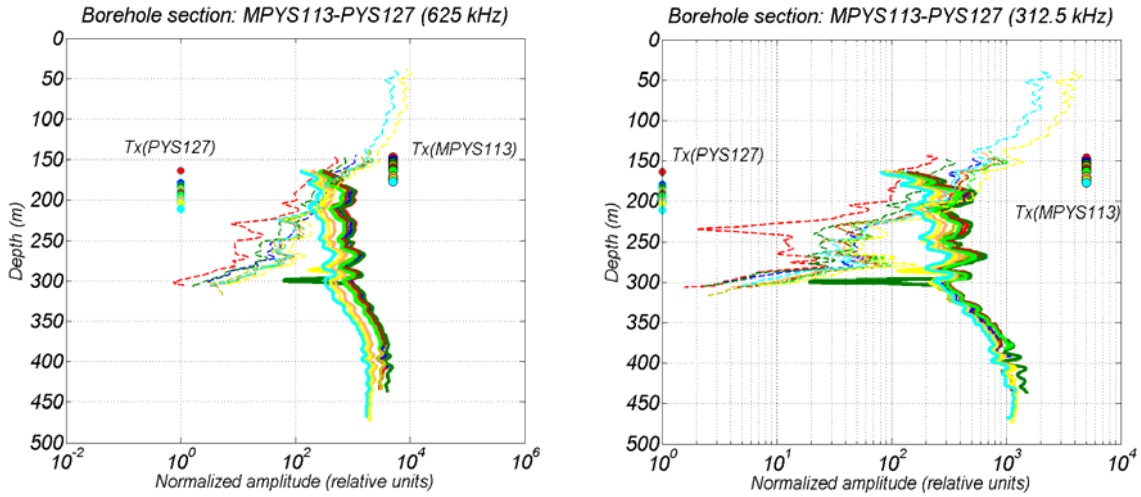

Figure 14. *The normalized amplitudes measured in boreholes PYS127 (bold lines) and MPYS113 (dashed lines). Corresponding transmitter positions marked are with coloured circles. Depths are real vertical depths.*

Plotting measured signals of both boreholes in same image (Figs. 13- 14) is a simple way to delineate possible targets in the section, i.e. to identify conductors or attenuators. It is evident that the attenuating material in the upper parts of the section must be situated close to borehole PYS127, effectively masking the transmitter in PYS127 (*dashed lines*) and having increasing amplitudes (*bold lines*) when the transmitter is situated in MPYS113. The depth of the anomaly ranges between 175 and 225 m. The final interpretation is based on a straight ray assumption (*zero wavelength*), or transmitted power is assumed to propagate along straight lines from the transmitter to the receiver. In Figure 15, the tomogram of borehole section MPYS113-PYS127 is presented (Korpisalo, 2010d).

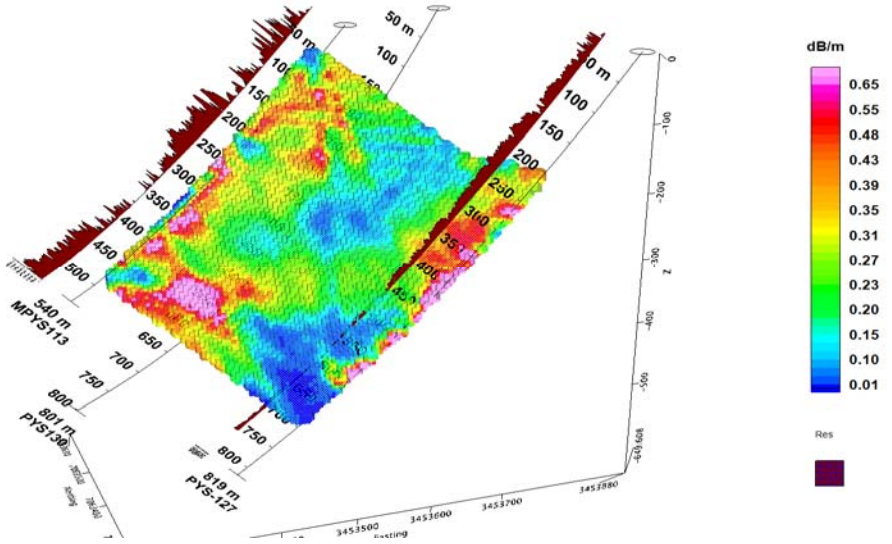

Figure 15. *A tomogram at a frequency of 625 kHz. Resistive logging results are displayed beside the boreholes as filled profiles (brown). In borehole MPYS113 the correlation between electric and RIM results is very good. Both have a strong contact with low resistivity (conductive) sections between 100-200 m and 300-400 m. In addition to common features of both methods, the cross-sectional image (tomogram) of RIM resolves a large and interesting attenuating material concentration near the borehole MPYS113 in the depth level of 400- 500 m. It is dipping slightly upwards towards PYS127 where both methods have contact with a low resistivity section between 300- 400 m. The concentration seems to broaden downwards towards the borehole PYS127.*

6.1 Comparison of electric resistive borehole logging and RIM registration

Electrical resistivity logging of boreholes is an important, simple and efficient exploration technique in identifying mineralised zones or sometimes graphite in a close proximity to a borehole wall (Fig. 15) (Parasnis, 1986). It is usually the first logging method used on a new borehole and is considered to be a primary logging method on which further logging is based. The measurement of resistivity is related to the conductive rock materials near the borehole. Direct or low-frequency alternating current is fed into the ground using two current electrodes. The resulting potential difference is measured by two voltage electrodes to provide information about the apparent electrical resistivity surrounding the borehole. Typical borehole logging systems provide short normal and long normal resistivity measurements. The advantage of long spacing is that resistivity is measured deeper into the formation, while the advantage of short spacing is that thin beds are better defined.

Resistivity logging results in boreholes MPYS113 and PYS127 and EMRE registrations (*relative units*) in section are displayed in Figures 16-17. The results for signals from transmitter in PYS127 measured in MPYS113 are presented in Figure 16. The resistivity data reveals a strong contact with fairly conductive material in the upper parts of MPYS113 (*150-200 m)*. Respectively, the amplitudes (*relative units*) are at very low levels (*<10000 units*) in the same depth range but mostly have more of declining trend below 200 m, meaning an increase in attenuating material between the boreholes. A brief increase in amplitudes at the level of 200-220 m is followed by the same trend but more emphasized in upper receiver positions. A sudden and local decrease in amplitudes just before the level of 300 m correlates well with the resistivity data. Below the 300 m level, amplitudes further decrease and are at the level of noise at 350 m (*upper receiver positions*). This is followed by an increase in amplitudes at depths of up to 400 m before a sudden decrease to the noise level, indicating the receiver being effectively shadowed by conductive material, perhaps attenuating material having a slightly dipping trend downwards to-

wards the deeper parts of borehole PYS127. A strong contact with low resistivity material is also evident at the 350-400 m level. Contrary to amplitudes, resistivity values remain at fairly high levels below 400 m.

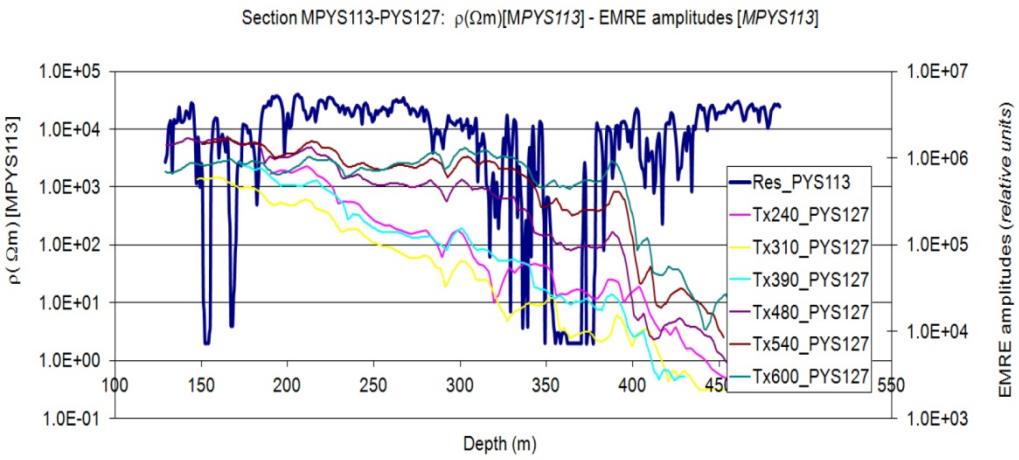

Figure 16. *EMRE signals from borehole PYS127 (stations 240 m, 310 m, 390 m, 480 m, 540 m and 600 m), measured in PYS113 and resistivity registration in PYS113 (blue). Low resistivity sections 350-380 m and 400-450 m also indicate changes in amplitudes. The low resistivity section from 150–180 m is not visible in EMRE signals.*

The reverse measurements from PYS127 with the transmitter in MPYS113 indicate rather similar behaviour (Fig. 17) and confirm the assumptions made before changing the transmitter. The resistivity values are at a fairly high level. There are some local references from low resistivity material above the 300 m level, but the first perceptible effects of the conductive material can be seen at the levels of 300-325, 350-400 and 450-475 m. Above 300 m, amplitudes are at low levels, after which they follow slightly increasing trends, meaning that attenuating material between the holes might be dipping downwards from MPYS113 towards PYS127, as was concluded before changing the transmitter between boreholes. In the upper transmitter positions (*Tx210 and Tx240*), the effect of attenuating material between the boreholes decreases, until the amplitudes follow a sudden decreasing trend at 220 m. At deeper transmitter positions the decrease in

amplitudes is also visible and happens later. Amplitudes start to increase below the level of 250 m in upper transmitter positions and later in deeper positions meaning, that resistive material could be dipping downwards from PYS127 towards the lower parts of MPYS113.

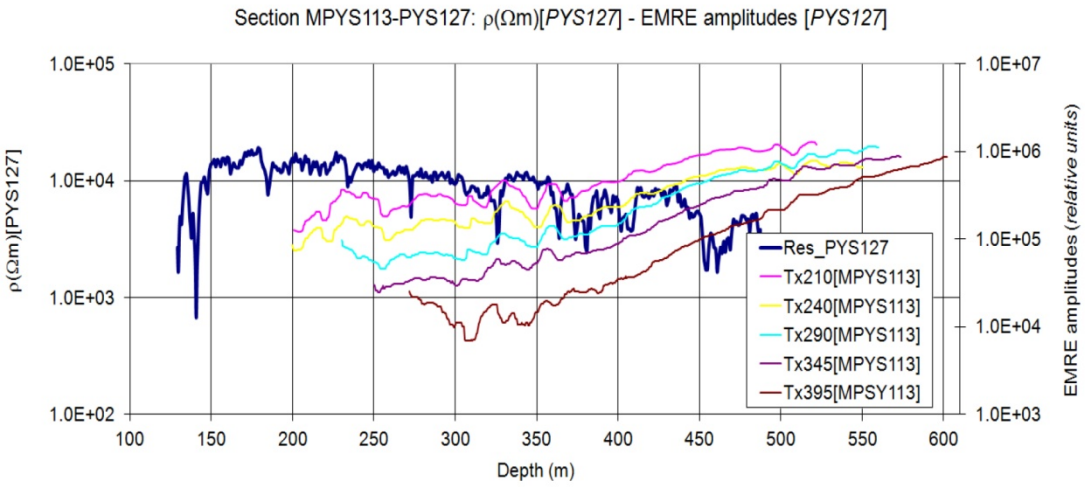

Figure 17. *EMRE signals from borehole PYS113 (stations 210 m, 240 m, 290 m, 345 m and 395 m) measured in PYS127 and resistivity in PYS127. Low resistivity sections from 300–430 m also indicate changes in amplitudes. However, the low resistivity section at 450 m is not visible in EMRE signals.*

As a conclusion RIM measurements have the same distinct and even highly localized features as electric logging data (*350-380 m*) in MPYS113 (Fig. 16), but one has to remember that electric logging senses the close vicinities of boreholes and EMRE signals result from geological formations in the first Fresnel zone volume between the boreholes (Korpisalo, 2010c). Besides, in upper parts (*at ~170 m*), electric logging in PYS127 (Fig. 17) has a strong localized reference to a low resistivity section (*not in the range of RIM measurement*), but the effect can be seen in Figures 12-13, where amplitudes are at a diminished level. Again, at a depth of ~400 m, electric logging in MPYS113 (Fig. 16) has contact with a low resistivity section, which can also be weakly seen in EMRE signals in Figures 14-15 (*bold line*s) and Figures 11-12. Thus, radio wave attenuation in rocks corresponds to electrical conductivity, but it is not only the changes in the

attenuation constant that increase or decrease the measured signal levels. The relationship between the antennas and the borehole environment may change greatly from point to point, having an effect, for instance, on the scattering parameter s_{11} (Fig. 9), polarization losses, and reflection/scattering losses, on signal levels being combined with the material attenuation (Korpisalo, 2010a).

6.2 Comparison of borehole TEM measurement and RIM registration

The transient electromagnetic method (*TEM*) is an EM method functioning in the time domain, in contrast to frequency domain methods (*e.g. RIM/EMRE*). Using TEM, the electrical resistivity of the underground layers can be measured down to a depth of several hundreds of metres. The principle of TEM is simple and is based on the fact that when current is flowing in a transmitter loop it sets up a magnetic field, and after the current is switched off the magnetic field induces eddy currents to flow in an electrical conductor in the ground. The eddy currents set up a secondary magnetic field, which can be detected by a 3-component (H_x, H_y, H_z) receiver loop as a time-dependent decaying voltage. The induced receiver voltage will therefore provide information on the resistivity as a function of depth. The datasets are recorded in decay time windows, known as gates. The gates are arranged with a logarithmically increasing width to improve the signal/noise (*S/N*) ratio, especially at later times (Nabighian & Macnae, 1991).

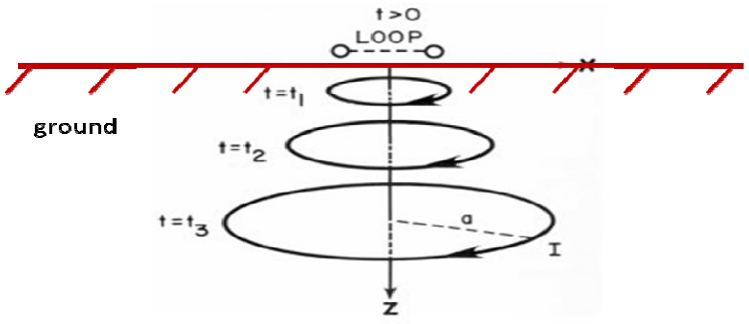

Figure 18. *Propagation of currents underground as "smoke rings" (Nabighian & Macnae, 1991).*

The propagation of the current into ground is represented in Figure 18 as "smoke rings". The current induced in the ground after switching off the transmitter current is shown for different times. Typical measuring times are in the range of micro- to milliseconds. Results from transient PROTEM measurements in borehole MPYS113 are presented in Figure 19. The corresponding measurements were also carried out in PYS127 and the results are presented in Figure 20.

Borehole MPYS113

a)

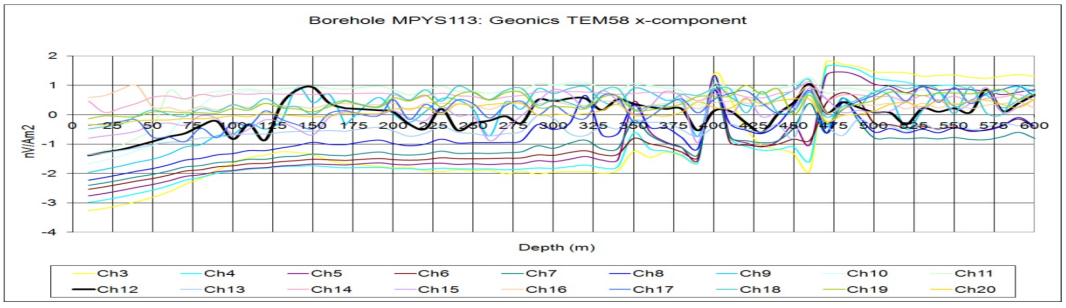

b)

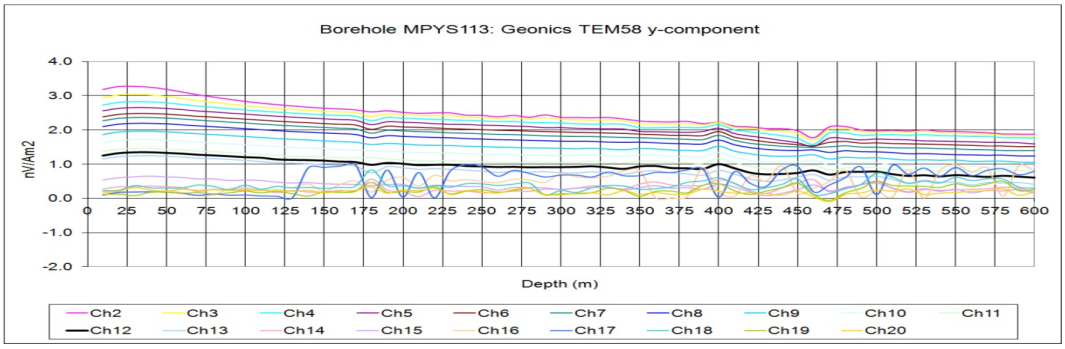

c)

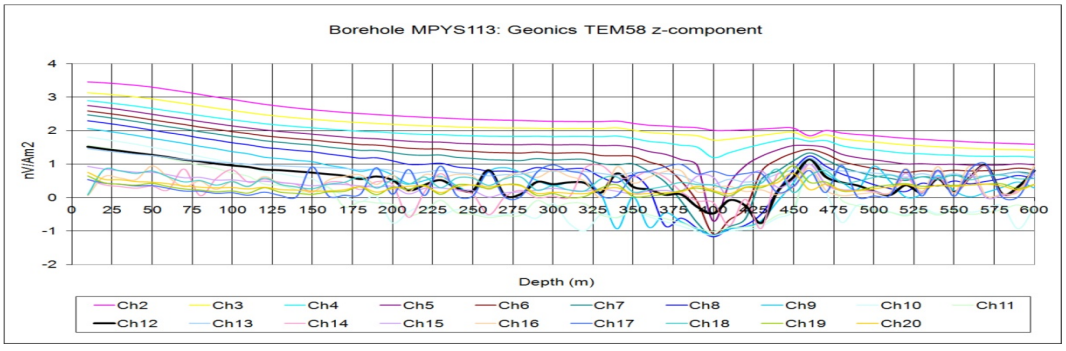

Figure 19. *PROTEM measurement in borehole MPYS113. a) x-component, b) y-component and c) z-component. The induced voltages are normalized by the current and transmitter loop area (nV/Am^2).*

The intensities of all components are at the same levels (Fig. 19). The early channels of the x-component are purely negative whereas the y- and z-components have positive early channel intensities. In all components, early channel intensities indicate resistive ground at moderate depths. In later channels the x-component oscillates from -1 to +1 nV/Am^2, indicating that outside of the borehole an (*elongated*) conductive body could be situated more tangential in the x-axis direction, as is the case with the z-component. Both components (*x and z*) react to the upper surface of the conductor at the level of 350 m. The lower surface of the conductor reaches down to the 500 m level. The same effect is clearly visible in tomogram (Fig. 15).

Borehole PYS127

a)

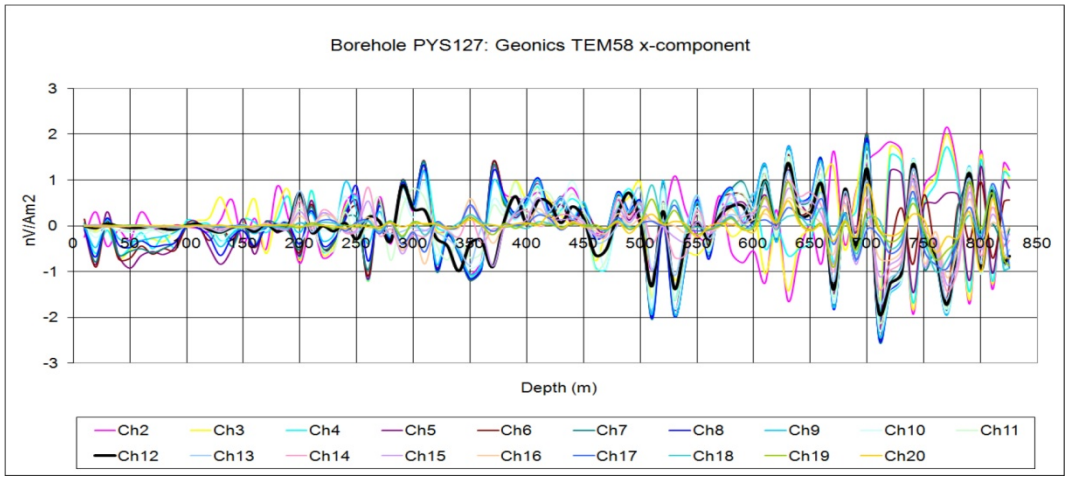

b)

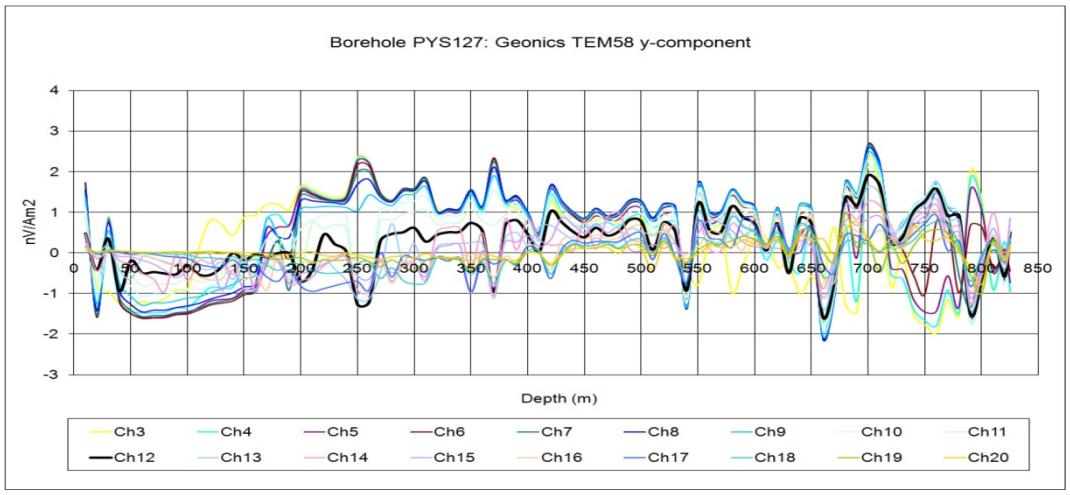

c) 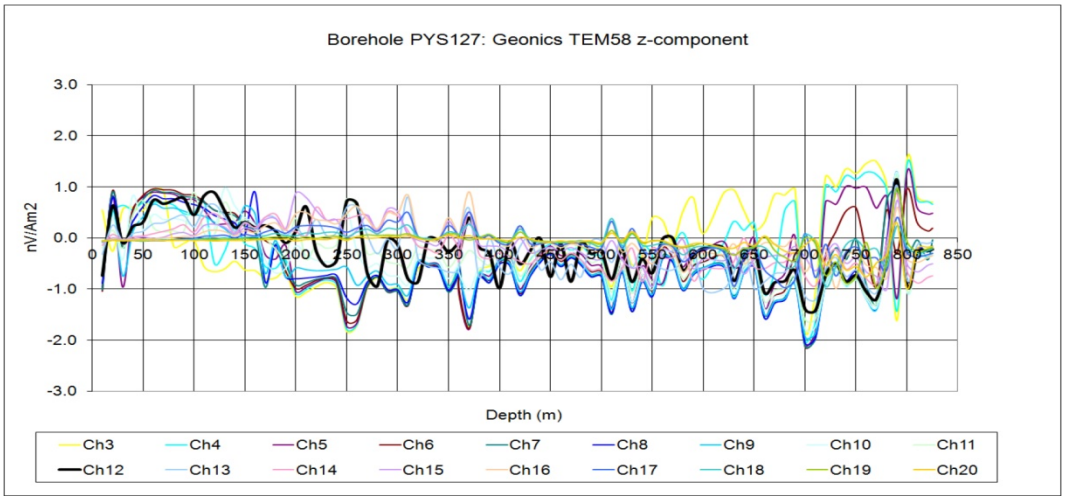

Figure 20. *PROTEM measurement in borehole PYS127. a) x-component, b) y-component and c) z-component. The induced voltages are normalized by the current and transmitter loop area (nV/Am^2).*

The intensities of the components vary, the x- and z-components being at lower levels (Fig. 19). The y-component has the highest intensities, so y-axis might be situated in a more perpendicular position with a conductor outside the borehole. In the early channels, both the y- and z-components give a strong indication of the upper surface of the conductor, starting from the level of 200 m, diminishing at 500 m and becoming stronger again at deeper levels. This indicates the conductor position in the depth interval of 200-500 m, which is also visible in the tomogram (Fig. 15).

6.3 Repeatability of results with the EMRE device

The repeatability of registrations is one of the most important characteristics of a good device, and it is reasonable to occasionally take some re-measurements during fieldworks. The good repeatability of our device can already be seen in Figures 13-14, where the transmitter steps were 5 meters, and it is reasonable to assume that the geology does not generate very strong changes in the signals when frequencies of 312.5- 2500 kHz are used with short steps. Figure 21 presents the results of a quality test carried out to ensure the functioning of the system, and one transmitter position is repeated on successive days. The result is excellent taking into account that the accumulation levels of batteries may have been different and there may have been a slight error in transmitter positions.

a)

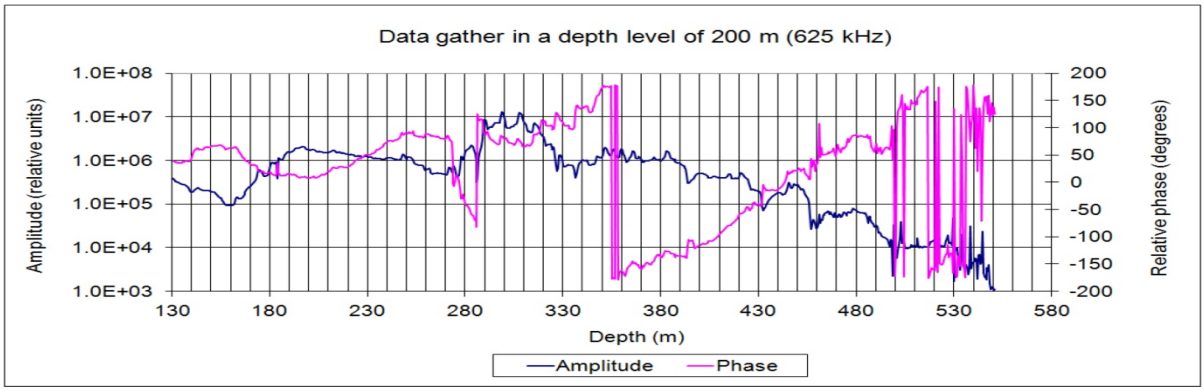

b)

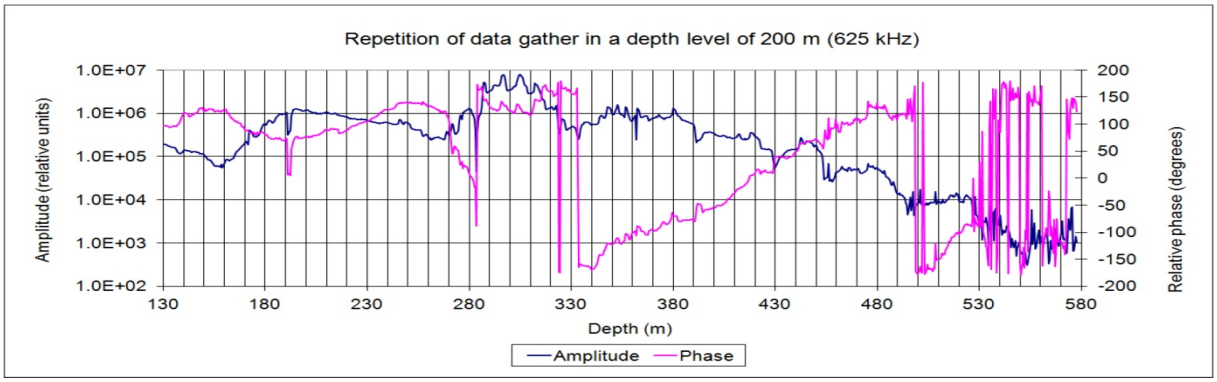

Figure 21. *a)* Original measurement. *b) Re-measurement in one transmitter position. There is a slight difference in the amplitude level between measurements because of the different accumulation levels of batteries, or the transmitter may have been in a slightly different position.*

7 DISCUSSION AND CONCLUSION

This paper illustrates our first experiences with a geophysical borehole exploration technique known as RIM (*Radio Imaging Method*). The first trials to examine the penetration of electromagnetic waves into rocks were performed at the beginning of the 1900's to determine whether the penetration is sufficient and measurements could be useful in exploration of the geophysical properties of rocks. After decades of development in the basic theory, increased understanding of material response to the electromagnetic waves and new electronic solutions, are the basement that transmitted radio waves can now be registered in a remote receiver and a tomographic reconstruction of borehole section (*attenuation distribution*) can be performed.

The first results and experiences with RIM (*the EMRE system*) have now been gained in the real field situations. The device has functioned well and both the amplitudes and phase differences have been recorded. The penetration ranges depend on several factors but in resistive environment and at the lowest measurement frequency (*312.5 kHz*), the borehole distances can be as large as 1000 m, while in more conductive conditions, the borehole distances of 400-600 m can be reached with the whole frequency band (Korpisalo, 2010b). The transmitter antennas are 20/40 m long. Thus, the requirement for the sufficient transmitter step is on a same scale. It may be reasonable to use shorter steps in the upper and lower edges of the sections which are the potential sources of artefacts in the tomograms. The measurement frequency of the receiver is 2 Hz meaning a receiver step size of ~0.4-0.5 m. Thus, for instance, the scanning length of 350 m can consist of 700 receiver positions. The weakest measurable signal level or the sensitivity of receiver is about ~0.5 μV and the phase resolution is about 10 degrees. The dynamic power range of the receiver is < 40 dB, being a restrictive property, and the user has to carefully control the recording levels during the measurements. If the amplitude levels are too high (*near saturation*), the system is going to be used in a section where the boreholes are too close to each other, and

antenna effectiveness has to be reduced by perhaps changing the antenna to shorter one or with jumper settings, a harmful frequency or frequencies must be rejected from the normal operation.

When comparing the resistivity logging results and the amplitude signals of RIM in borehole *MPYS113* (*Fig 16*), it was found that the electromagnetic method could reveal the same and even highly localized anomalies. This is a result of the strong influence of conductive material on the impedance of antennas. Monitoring the antenna impedance of transmitter, can be an effective means to discover anomalies near the boreholes. The results from TEM (Figs. 19- 20) were in close agreement with RIM, especially in borehole MPYS113 (Fig. 19), where a highly conductive and massive region could be localized with both methods. The indication was not as strong in TEM, perhaps TEM lost its sensitivity in the depth range and/or a massive 3D-region had complicated effects on the TEM signals.

RIM and the resistivity logging method gives the same results under certain circumstances (Fig. 16), the conductive zone near the borehole must be massive enough to be detectable with RIM, but located a little further from the borehole, the logging loses its sensitivity but RIM's ability is even enhanced. When comparing TEM and RIM, the conductive anomaly can be located reliably by the both methods. However, when distance from the boreholes increases over few hundreds of metres, TEM loses its sensitivity. The depth dimension can also be a restrictive issue with TEM if the loop size cannot be increased. On the contrary, RIM can be used all along the borehole and at the distances where the boreholes are separated by even one thousand metres. Thus, RIM can offer higher resolution than TEM, both due to its higher frequencies and because the RIM transmitter is lowered down a borehole, closer to the targets, compared to a large surface transmitter loop.

According to our first experiments with RIM, it is evident that radio waves can penetrate sufficiently into rocks and useful measurements can be made to determine the physical properties of rocks (Korpisalo, 2010b). A cross-borehole EM survey has several clear benefits over ground-

level electromagnetic sounding methods. Applying a borehole source, it brings the survey closer to the target, and will allow the use of higher frequencies, thus enabling a higher spatial resolution. Another benefit is the possibility to view the target from different angles and directions not only in the vertical direction. Having the source in a borehole eliminates the boundary effects related to the ground surface and the strong attenuation emerging from soil deposits. A drawback is the suboptimal availability and location of the boreholes.

Inspired by these promising results, the development of the EMRE system is under consideration, and an additional high frequency option (*5000 kHz*) is going to be added to the system. Both the transmitter and receiver will be designed to work more effectively. Weaker signals (~0.1 μV) should be detectable and a broader dynamic range of 60 dB would increase the usefulness of the device. The angular resolution of the present device is ~10 degrees, but a resolution of <2 degrees is possible. These improvements can be performed, e.g. by improving the frequency synthesis and minimizing phase losses using temperature compensated crystal oscillators (*TXCO*) both in the transmitter and receiver. TXCO have components that will compensate for changes in ambient temperature and keep the oscillator on frequency. Otherwise, variations in temperature would vary the crystal frequency up or down, which is a disturbing feature in the present equipment. In addition, to improve the operation level of the receiver, the present mixer technique must be modernized and followed by an effective filter stage. With developments of this kind, the EMRE system could become a powerful tool in large rock building projects to more precisely determine the structural integrity of the rock. At present, amplitude data are utilized. However, the relative phase difference contains information on the relative permittivity. Thus, the development of phase interpretation is also under consideration.

8 ACKNOWLEDGEMENTS

I wish to acknowledge RF-specialist Mika Niemelä who maintained the proper functioning of the EMRE device. I would especially like to thank geophysicist Hannu Hongisto for insightful comments and advice on TEM measurements. Professor Lauri Pesonen (*Helsinki University*) and geophysicists Kimmo Korhonen and Tapio Ruotoistenmäki (*Geological Survey of Finland*) greatly aided in the preparation of this paper.

9 REFERENCES

Buselli G., 1980, Electrical geophysics in the USSR, Geophysics, vol. 45, n: 10, 1551-1562.

Dines K., 1979, Computerized Geophysical Tomography, Proceeding of IEEE, vol. 67, no: 7.

Holloway G. L., 1998. Radio-Frequency Communication Principles, Published by Naval education and training professional development and technology center, NAVEDTRA 14189. Module 17.

*Junxing Cao, Zhenhua He, Jieshou Zhu, Peter K Fullagar***,** 2003. Conductivity tomography at two frequencies. Geophysics 68, 516.

Korpisalo A., 2010a, Borehole antenna considerations in the EMRE system: Frequency band 312.5 – 5000 kHz. (unpublished, part of PhD thesis).

Korpisalo A., 2010b, EMRE electromagnetic radiofrequency imaging system: Instrumentation and method. (unpublished, part of PhD thesis).

Korpisalo A., 2010d, RIM measurements in three borehole sections at Pyhäsalmi area with EMRE system, 2008. (unpublished, part of PhD thesis).

Korpisalo A. and Niemelä M., 2010e, Cross-borehole Research with EMRE-System: Radiofrequency Measurements in Drillhole Section OL-KR-40-OL-K45 at Olkiluoto, 2009. Posiva working report 2010-24.

Korpisalo A. and Niemelä M., 2010e, Cross-borehole Research with EMRE-System: Radiofrequency Measurements in Drillhole Section OL-KR-40-OL-K45 at Olkiluoto, 2009. Posiva working report 2010-24.

Korpisalo A., Jokinen T., Popov N., Shuval-Sergeev A., Zhienbaev T., Heikkinen E., Nummela J., 2008, Review of Crosshole Radiowave Imaging (FARA) in drillhole sections OL-KR4-OL-KR10 and OL-KR10-OL-KR2 in Olkiluoto, 2005. Posiva working report 2008-79.

Korpisalo A., 2007, FARA –laitteen kokoonpano ja käyttö, Geological Survey of Finland, Archive report, (in Finish), Q15/2007/13.

Kousa J., Marttila E. and Vaasjoki M. 1994. Petrology, geochemistry and dating of Paleoproterozoic metavolcanic rocks in the Pyhäjärvi area, central Finland. Geological Survey of Finland, Special paper 19, 7-27.

*Mäki T. 1986***,** Lithogeochemistry of the Pyhäsalmi zinc-copper-pyrite deposit, Finland. In: Prospecting in areas of glaciated terrain symposium, Sept. 1-2, 1986 Kuopio, Finland. London: IMM, 69-82.

Nabighian M. N. and Macnae J. C., 1991, Time domain electromagnetic prospecting methods, in Nabighian, M. N., Ed., Electromagnetic methods in applied geophysics, Vol II, Part A: Soc. Expl. Geophysics, 427-509.

Parasnis D. S., 1986, Principles of Applied Geophysiscs. Fourth edition. Chapman and Hall, London.

Redko G. V., Lebedkin L. V., Shuval–Sergeev A., Popov N., Stevens K. and Kazda G., 2000b. Borehole electromagnetic geophysical methods in ore and coal deposits. A paper at the International Conference "300 years of Russian mine–geological service", Saint–Petersburg (Russia), 2000.

G.V. Redko, K.D. Ratnikov, A.P. Savitsky, A.B. Fedorov, A.N. Shuval-Sergeev, 2000a. The Radiowave Method Applied To Ore Deposits. http://www.farasystem.ru/Pubs/Spb2000_Abstr_E.pdf.

Stevens K, Watts A and Redko G, 1998, In–Mine Applications of the Radio–Wave Method in the Sudbury Igneous Complex. A paper at the International Conference "Mine Geophysics–98", Saint Petersburg (Russia).

Smith G. S., 1997, An introduction to classical electromagnetic radiation. Cambridge University Press.

Stolarczyk L. G. and Fry R. C., 1986, Radio imaging method (RIM) or diagnostic imaging of anomalous geologic structures in coal seam waveguides. *Transactions* of Society for Mining, Metallurgy, and Exploration, Inc., *Vol. 288*, 1806-1814.

Vogt D,2000, The modelling and design of Radio Tomography antennas, DPhil thesis, unpublished, University of York (United Kingdom), http://www.opengrey.eu/item/display/10068/624370.